Amphiphilic Gold Nanoparticles Grafted with Poly(*N*-isopropylacrylamide) and Polystyrene

Jun Shan,[†] Markus Nuopponen,[†] Hua Jiang,[‡] Tapani Viitala,[§] Esko Kauppinen,[‡] Kyösti Kontturi,[⊥] and Heikki Tenhu*,[†]

Laboratory of Polymer Chemistry, University of Helsinki, PB 55, FIN-00014 HY, Finland; VTT Processes, Materials and Chemicals, PB 1602, FIN-02044 VTT, Finland; KSV Instruments Ltd., Höyläämötie, FIN-00380 Helsinki, Finland; and Laboratory of Physical Chemistry and Electrochemistry, Helsinki University of Technology, PB 6100, FIN-02015 HUT, Finland

Received April 15, 2004; Revised Manuscript Received December 21, 2004

ABSTRACT: Two types of amphiphilic gold nanoparticles (AuNP-1 and -2) grafted with a mixture of poly(*N*-isopropylacrylamide) (PNIPAM) and polystyrene (PS) chains in two different compositions have been successfully prepared with the "grafting-to" method in a homogeneous THF phase. These AuNPs were thoroughly characterized by FTIR, ^{1}H NMR, UV−vis, high-resolution transmission electron microscopy, thermogravimetric analysis, and dynamic light scattering to determine the total number of polymer chains bound to the gold nanoparticles, the ratio between PNIPAM and PS chains, and the size of the gold core. Langmuir monolayer experiments at the air−water interface of the two types of AuNPs revealed different compression isotherms of the surface pressure vs particle area (π−A curve) conducted at 20 °C. These amphiphilic gold nanoparticles can be regarded as analogues of amphiphilic diblock copolymers at the air−water interface. The compression isotherm of AuNP-2 with a PNIPAM:PS ratio of 2:1 showed several characteristic regions that can be attributed to the polymer conformational transitions from the pancake, the pancake to brush transition, to the brush. However, the monolayer of AuNP-1, with a ratio of 5:1 of PNIPAM:PS, never reaches a brush stage but showed an extension of the pseudoplateau region upon compression. These differences may be due to the more hydrophilic nature and the more stretched PNIPAM chains. Furthermore, the sessile drop contact angle measurements, conducted at room temperature on both upper and lower surfaces of the AuNP-2 monolayer transferred at 35 mN/m onto either hydrophilic or hydrophobic substrates, are slightly different, 82 ± 2° and 77 ± 2°, respectively. After comparing with the literature data of the contact angles of water on either the pure PS film or the PNIPAM brush, we concluded that the chemically different PNIPAM and PS chains grafted on the surface of the gold core tend to be phase-separated.

Introduction

Functionalized gold nanoparticles have attracted great interest during the past decade due to their potential applications in biomedical, electronic, and optical materials as well as in catalysis.[1−3] Only noble metals like gold are capable of existing in the unoxidized state at the nanoscale and offer a unique surface chemistry that allows them to be used as platforms for self-assembly layers of organic molecules.[4] Inspired by a reliable and facile synthesis method of preparing alkanethiol-protected gold nanoparticles reported by Brust,[5] monolayer-protected gold nanoparticles grafted with polymers have subsequently been developed in recent years.

Although there are a variety of ways to prepare highly dense polymer brushes onto metal nanoparticles which possess long-term stability and can repeatedly be isolated and redissolved, mainly two different techniques are commonly used, i.e., "grafting-from"[6−9] and "grafting-to".[10−14] The "grafting-from" technique allows polymers to be built up at the surface of the gold nanoparticles using a surface-confined polymerization. So far, several researchers have utilized the "grafting-from" technique to prepare gold nanoparticles grafted with polymers, like poly(methyl methacrylate),[6,7] poly(*n*-butyl acrylate),[8] and poly(*N*-isopropylacrylamide).[9] Alternatively, using the "grafting-to" technique, grafted gold nanoparticles can be prepared in situ in a homogeneous solution consisting of $HAuCl_4 \cdot xH_2O$ and polymers end-capped with functionalized groups. So far, gold nanoparticles passivated by thiolated poly(ethylene glycol),[10] thiol end-capped polystyrene,[11] and nonionic hydrophilic polymers containing disulfide group anchors[12] have been reported. In our previous work,[13] PNIPAMs terminated with a thiol group or even with a dithioester were used to prepare gold nanoparticles by the "grafting-to" technique. Especially, we found that polymers bearing a dithioester end group synthesized through the reversible addition−fragmentation chain transfer (RAFT) polymerization can straightforward be employed in the synthesis of grafted gold nanoparticles, with no need of prehydrolysis of the polymers to the thiolated ones. This is because a dithioester end group can be reduced to a thiol simultaneously when reducing $HAuCl_4$ by adding a reductant.[14]

Recently, a topic of considerable interest has been how to organize the particles into an ordered two- or three-dimensional array. A striking feature of alkanethiol-stabilized gold and other metal nanoparticles is that they tend to spontaneously form highly ordered and closely packed superlattices, simply by spreading an organic solution containing the nanoparticles on a suitable substrate and then allowing a controlled evaporation of the organic solvent.[15] Several reports have

[†] University of Helsinki.
[‡] VTT Processes, Materials and Chemicals.
[§] KSV Instruments Ltd.
[⊥] Helsinki University of Technology.
* Corresponding author: Tel +358-9-19150334; Fax +358-9-19150330; e-mail Heikki.Tenhu@helsinki.fi.

10.1021/ma049269j CCC: $30.25
Published on Web 02/19/2005

Scheme 1. Preparation of Gold Nanoparticles Grafted with PNIPAM and PS Chains and Structures of Corresponding Homopolymers

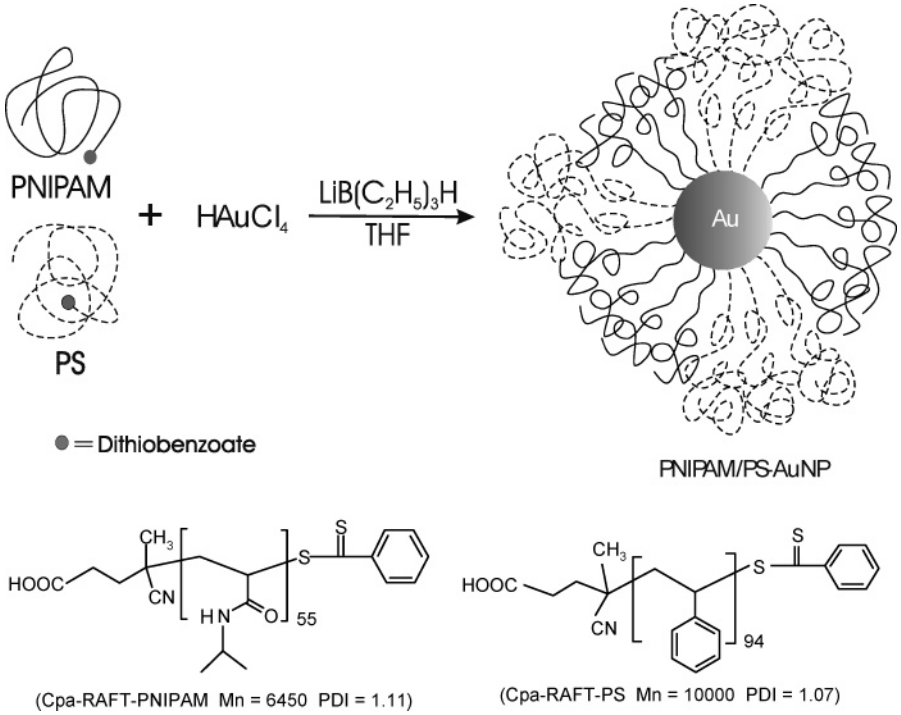

revealed that, by using the Langmuir−Blodgett (LB) film balance, either alkanethiol- or polymer-capped nanoparticles[16−18] can form stable monolayers at the air−water interface. This has further enabled the transfer of these nanoparticles to solid substrates, giving the possibility to study the quantized charge transfer.[19]

In this work we have for the first time successfully prepared amphiphilic gold nanoparticles grafted with a mixture of hydrophilic PNIPAM and hydrophobic PS chains by using the "grafting-to" technique. The monolayer behavior of the amphiphilic gold nanoparticles at the air−water interface was studied with a Langmuir film balance. Furthermore, sessile drop contact angle measurements on the deposited monolayers of the amphiphilic gold nanoparticles were performed to analyze the distribution of chemically different polymer chains on the surface of the gold cores.

Experimental Section

Chemicals. *N*-Isopropylacrylamide (NIPAM, Polyscience Ins.) was recrystallized twice from benzene. Styrene (Aldrich) was distilled under reduced pressure prior to use. Hydrogen tetrachloroaureate(III) hydrate ($HAuCl_4 \cdot xH_2O$, Au content: 52%, Fluka), 1.0 M solution of lithium triethylborohydride ($LiB(C_2H_5)_3H$) in THF (Aldrich), and 4,4′-azobis(4-cyanopentanoic acid) (ACPA, Fluka) were used as received. 2,2′-Azobis(isobutyronitrile) (AIBN, Fluka) was recrystallized from methanol. Tetrahydrofuran (THF) (Lab-Scan, HPLC) used for the synthesis of gold nanoparticles was dried by refluxing over calcium hydride and freshly distilled prior to use. Dioxane (Lab-Scan, Analytical Ac.) was distilled before use. Sodium methoxide solution in methanol (∼30%, 5.4 M, Fluka), benzyl chloride, elemental sulfur, and alumina (Merck) were used as received. The water used for all the measurements was purified and deionized in an Elgastat UHQ-PS purification system.

Synthesis of PNIPAM and PS by RAFT Polymerization. PNIPAM and PS were synthesized by RAFT polymerization starting from the preparation of a RAFT agent, 4-cyanopentanoic acid dithiobenzoate (cpa-RAFT).[20,21] The synthetic routes have been reported earlier.[22] Here the synthesis of cpa-RAFT-PNIPAM is described in brief. 12 g of NIPAM monomer (1.77 M), 150 mg of cpa-RAFT agent (8.95 mM), and 6.4 mg of AIBN (0.65 mM) were dissolved in 60 mL of dioxane in a round-bottom flask equipped with a magnetic stirrer. The mixture was degassed by four freeze−pump−thaw cycles, sealed under vacuum, and polymerized in a thermostated oil bath at 60 °C for 48 h. The polymer was precipitated in excess of diethyl ether, purified by repeated precipitations, and dried under vacuum.

PS was synthesized with a route similar to that for PNIPAM, except for the concentration of styrene monomer of 6.4 M, cpa-RAFT agent 3.6 mM, AIBN 0.47 mM, and the volume of the solvent dioxane of 15 mL. After polymerization, the reaction mixture was dissolved in THF, and PS was precipitated in cold methanol, purified by repeated precipitations, and dried in a vacuum. The molar masses (M_n, g/mol) and polydispersities (PDI) of PNIPAM and PS, measured by size exclusion chromatography (SEC), are shown in Scheme 1.

Preparation of Amphiphilic Gold Nanoparticles. AuNP-1 and -2 were prepared in a homogeneous THF phase, using the "grafting-to" technique (Scheme 1). The concentration of $HAuCl_4 \cdot xH_2O$ was 0.005 M (0.1 mmol in 20 mL of THF) in each recipe, with a molar ratio of 10/1 for $LiB(C_2H_5)_3H$/$HAuCl_4 \cdot xH_2O$ in the preparation of each AuNP. As an example, the preparation of AuNP-1 is described in detail below. To a vigorously stirred yellow solution of 0.1 mmol (37.9 mg) of $HAuCl_4 \cdot xH_2O$ in 10 mL of anhydrous THF was added a solution containing 0.01 mmol (64.5 mg) of PNIPAM and 0.01 mmol (100 mg) of PS dissolved in 10 mL of anhydrous THF (the molar ratio PNIPAM:PS:$HAuCl_4 \cdot xH_2O$ = 1:1:10). The mixture was stirred for 20 min in an ice bath. Then, 1.2 mL of 1.0 M THF solution of $LiB(C_2H_5)_3H$ was added dropwise in 2 min to the vigorously stirred solution. The solution immediately turned purple with a little gas evolution and was stirred for further 4 h. The supernatant was first separated from the precipitate by a centrifuge at 15 000 rpm. Only a small amount of precipitate was observed on the bottom of the centrifuge tube, and the supernatant was collected. THF in the supernatant was removed with a rotary evaporator. The purple crude product was dispersed in ethanol (99.5 wt %, Primalco Oy, Finland), and the dispersion was then purified by ultrafiltration using a membrane with molar mass cutoff

30 000 g/mol (Millipore, material: regenerated cellulose, filter code: PLTK, diameter: 47 mm) and ethanol as an eluent to remove the free PNIPAM. The product was further washed using diethyl ether five times to get rid of the free PS and dried in a vacuum. The received powder of AuNP-1 appeared purple. Another analogue, AuNP-2, also with a purple color, was prepared and purified using the same procedure except for the feed ratio, PNIPAM:PS:$HAuCl_4 \cdot xH_2O$ = 1:2:10.

Instrumentation and Characterization. Spectroscopy. FT-IR spectra of the two AuNPs and corresponding homopolymers of PNIPAM and PS were recorded in the range of 4000−650 cm^{-1} with a Perkin-Elmer Spectrum One. ^1H NMR measurements were conducted with a 200 MHz Varian Gemini 2000 spectrometer. Deuterated chloroform (99.90%D, Eurisotop, France) was used as a solvent to dissolve the synthetic PNIPAM sample for the estimation of its molar mass (the spectrum not shown). For the estimation of the molar ratio of PNIPAM/PS chains bound to the gold nanoparticles by ^1H NMR, the two AuNPs were dissolved in deuterated tetrahydrofuran (99.50%D, Euriso-top, France) (see the Results and Discussion section). UV−vis absorption spectra (400−800 nm) were recorded at 20 °C on a Shimadzu UV-1601PC spectrophotometer from the THF solutions of two AuNPs of ca. 0.65 mg/mL for the measurement of the surface plasmon band (SPB) of the AuNPs.

Size Exclusion Chromatography (SEC). The molar masses (M_n) and the polydispersities (PDI) of PNIPAM and PS were determined with a Waters liquid chromatography system equipped with a Waters 2410 differential refractometer as a detector. Three Styragel columns (HR2, HR4, and HR6) were used in series. A 50 μL aliquot of the sample was injected, and THF was used as an eluent at a flow rate of 0.8 mL/min at 30 °C. The calibration was carried out with polystyrene standards (Showa Denko). It is well-known that the determination of the molar mass of PNIPAM is problematic. However, with low molar mass polymers (MW < 5×10^4 g/mol) the method seems to be reliable. This was confirmed by estimating the molar mass of PNIPAM by ^1H NMR spectroscopy, based on the integral of a resonance of two protons (δ = 7.95 ppm, *o*-ArH) of the phenyl group[20,21] (a fragment of the cpa-RAFT agent) at one end of a PNIPAM chain and on the other integral of a lone proton (δ = 4.01 ppm) of the *N*-isopropyl group[23] in the repeating units of PNIPAM.

High-Resolution Transmission Electron Microscopy (HRTEM). HRTEM images were obtained with a Philips CM200FEG, working at an accelerating voltage of 200 kV. The point-to-point resolution was 0.24 nm. Images were recorded by a GATAN slow scan CCD camera. Samples were prepared by drop-casting one drop of the appropriately diluted cluster solution in THF onto the holey carbon film on copper grid (S147-4, 400 mesh Cu, Agar Scientific Ltd.) and dried in air. The size distribution of gold nanoparticles was measured from the enlarged photographs of the TEM images for at least 200 individual gold cores.

Thermogravimetric Analysis (TGA). The total amount of the polymer ligand on the gold core surface was determined by a Mettler Toledo TGA 850 in flowing nitrogen atmosphere at ca. 50 mL/min. Temperature was increased from 25 to 800 °C with a rate of 10 °C/min.

Dynamic Light Scattering (DLS). The mean diameter of the AuNP-2 dissolved in THF, a good solvent for both PNIPAM and PS, was determined by DLS. The measurement was conducted at 20 °C with a Brookhaven Instruments BI-200SM goniometer and a BI-9000AT digital correlator at 90°. The light source was Lexel 85 argon laser (514.5 nm, power 50 mW). The time correlation functions were analyzed with a Laplace inversion program (CONTIN). The concentration of the AuNP was 1.0 mg/mL. The solution was filtered through Millipore membrane (0.45 μm pore size).

Langmuir Monolayers. The monolayer properties of both AuNPs at the air−water interface were measured with a KSV Minitrough film balance system (KSV Instruments Ltd., Helsinki, Finland) at 20 °C. The monolayer was prepared by spreading drops of a dilute chloroform solution of AuNPs (0.2 mg/mL) at the air−water interface using a 50 μL Hamilton glass syringe. The subphase used was deionized water. The barrier speed during compression was 5 mm/min. The isotherms were plotted as surface pressure vs particle area by using the KSV Win LB software.

The monolayers of AuNP-2 were deposited from the air−water interface to either a hydrophilic SiO_2 substrate (the size: 30 × 15 × 2 mm, Okmetic, Finland) or a hydrophobic substrate (see the preparation in the next paragraph) to perform contact angle measurements. The monolayer was first compressed to a predefined surface pressure (35 mN/m), and then keeping the surface pressure constant for about 10 min, thus allowing the relaxation of polymer chains until the monolayer was stabilized. The film was then deposited either on a hydrophilic substrate by vertically lifting up the substrate (i.e., hydrophilic transfer) or on a hydrophobic substrate by dipping it into the subphase through the monolayer at the air−water interface (i.e., hydrophobic transfer) at a constant deposition speed of 5 mm/min, keeping the surface pressure constant. Therefore, two sides, i.e., both upper and lower surfaces, of the AuNP-2 monolayer were obtained with LB transfer according to either lifting up or dipping in a substrate and were then denoted as surface L and surface D, respectively. It is worth noting that the hydrophobically transferred film (i.e., surface D) was taken out of the subphase after first removing the residual monolayer from water surface and then lifting the transferred film up from the water subphase. The transfer of the monolayer was monitored by the transfer ratio, which was always between 0.8 and 1.0. However, since the monolayer of AuNP-1 could not be compressed to a sufficiently high surface pressure, it was not deposited onto the SiO_2 substrate.

A hydrophilic SiO_2 substrate was obtained by immersing it into concentrated HCl for 1 h and then into concentrated HNO_3 for 1 h and thereafter rinsing with pure ethanol and water. The contact angle of this hydrophilic substrate was 25 ± 1°. The hydrophobic substrate was prepared by immersing a hydrophilic SiO_2 substrate in a toluene solution of 5 mM octadecyltrichlorosilane for 2 min and then rinsed with pure ethanol and water. The contact angle measured for this substrate was 97 ± 1°.

Deposition of the monolayer for HRTEM measurement was achieved by Schaefer transfer, i.e., horizontally touching a copper grid (S147-4, 400 mesh Cu, Agar Scientific Ltd.) to the monolayer at the same surface pressure as above, 35 mN/m.

Sessile Drop Contact Angle Measurements. The static contact angles of sessile water drops on the deposited monolayers were measured at room temperature with a CAM 200 contact angle measurement instrument (KSV Instruments Ltd., Helsinki, Finland). The CAM 200 utilizes video capture and subsequent image analysis by axis-symmetric drop shape analysis (ADSA). The liquid used for determining the contact angles was deionized water with a surface tension of 72 mN/m at 25 °C. In this work, the contact angle values were taken at the initial point from which the CAM 200 began to work on a sessile water drop because the PNIPAM chains started to reorganize (e.g., dissolution into water) as soon as a water drop touched the monolayer (see the discussion of the "contact angle measurements" in the next section). At least three readings were taken on different parts of the monolayers and averaged.

X-ray Photoelectron Spectroscopy (XPS). Surface composition for both surface L and surface D was evaluated by a high-resolution photoelectron spectrometer (AXIS 165 by Kratos Analytical). Survey scans were recorded using monochromatic Al Kα irradiation, 1 eV step, and 80 eV analyzer pass energy. High-resolution regional spectra of C 1s and O 1s were recorded using monochromatic Al Kα irradiation, 0.1 eV step, and 20 eV analyzer pass energy. All spectra were collected at the electron takeoff of 90° from sample areas less than 1 mm^2 in diameter. Each sample was analyzed from at least three different points. During the data acquisition, the insulating sample surfaces were neutralized with slow thermal electrons (system patented by Kratos). Prior to data analysis, the binding energies of high-resolution measurements were charge corrected using the C−C component of C 1s signal at 285 eV as an internal standard.

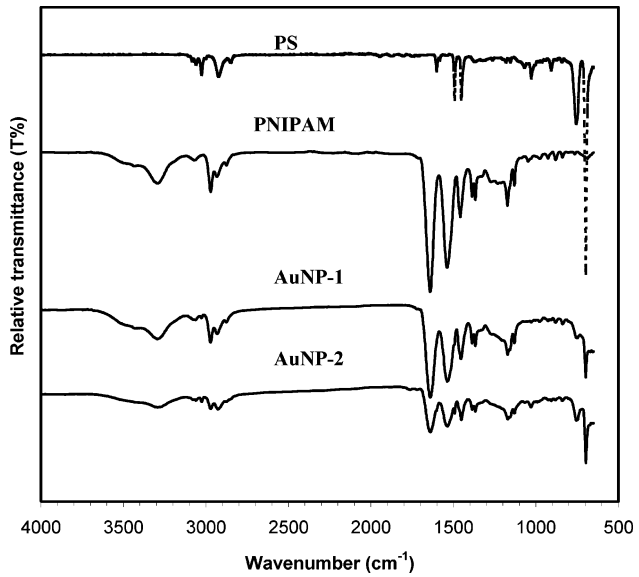

Figure 1. FTIR spectra of AuNP-1 and AuNP-2 and of two homopolymers PS and PNIPAM.

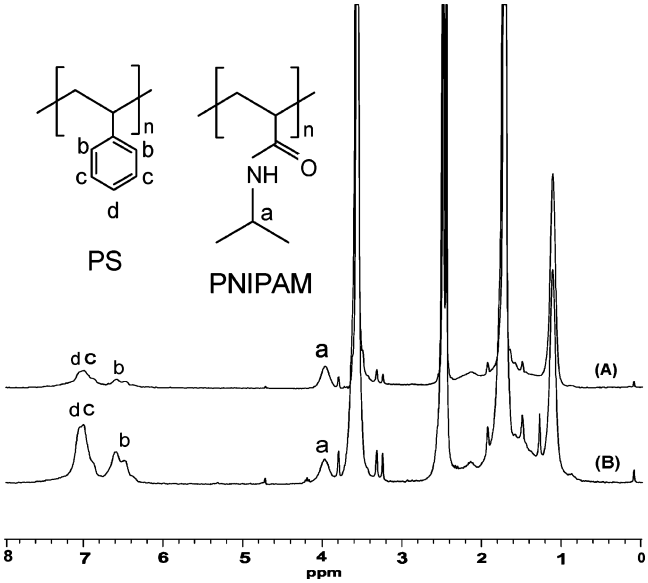

Figure 2. ^{1}H NMR spectra of (A) AuNP-1 and (B) AuNP-2.

Results and Discussion

Characterization of Both AuNPs. Figure 1 shows the FTIR spectra of the two AuNPs and the corresponding two homopolymers of PNIPAM and PS. The N−H stretching (3295 cm^{-1}), second amide C=O stretching (1640 cm^{-1}), second amide N−H stretching (1539 cm^{-1}), and deformation of two methyl groups (1386 and 1367 cm^{-1}) attributable to PNIPAM are clearly visible in the spectra of the AuNPs. On the other hand, the aromatic ring stretching (1455 cm^{-1}) and stretching of five adjacent H atoms in the benzene ring (756 and 697 cm^{-1}) can be attributed to PS. The FTIR results clearly show that both PNIPAM and PS are bound to the gold nanoparticles. This is also supported by the ^{1}H NMR spectra in Figure 2, in which the resonance labeled **a** (δ = 3.99 ppm) represents the lone proton of the *N*-isopropyl groups along the PNIPAM chains, and the resonances labeled **b**, **c**, and **d** ($\delta \sim$ 6.3−7.4 ppm) represent the five aromatic protons of the phenyl groups in PS chains. In the spectrum of (A), the integral of the resonance labeled **a** is 35.8%, and the total integral of the resonances labeled **b**, **c**, and **d** is 64.2%. In the spectrum of (B), the integrals are 16.7% and 83.3%, respectively. Based on both integrals in each spectrum, as well as the degrees of polymerization of PNIPAM and PS, the important molar grafting ratio parameter of PNIPAM/PS bound to the gold nanoparticles can eventually be calculated to be 5/1 and 2/1 for AuNP-1 and -2, respectively.

The mean diameters of the gold nanoparticles as received from HRTEM are 2.5 ± 0.7 nm for the AuNP-1 and 3.0 ± 1.0 nm for the AuNP-2 (Figure 3). The number of gold atoms contained per gold core and the surface area of each gold core can be obtained from the work by Murry on alkanethiol-protected gold nanoparticles.[24,25] These parameters are listed in Table 1. The shapes of the gold cores were taken as truncated octahedra as suggested by Whetten.[26,27] The total mass loss or the mass loss fraction of the polymer chains bound to the gold cores can be determined by TGA, but the respective mass loss fractions of the PNIPAM and the PS chains cannot separately be recognized from the thermogravimetric curve. This is because both PNIPAM and PS show thermal decomposition in the same temperature range of 220−460 °C. However, the respective mass loss fractions of the PNIPAM and the PS chains can be calculated by combining the molar grafting ratio obtained by ^{1}H NMR, the total mass loss fraction of the polymers obtained from TGA, as well as the molar masses of both PNIPAM and PS. Hence, they are listed in Table 1 for the two AuNPs. The respective numbers of the PNIPAM and the PS chains bound to a single gold core can hence be figured out by use of the molar grafting ratio and the number of the gold cores derived from the residue of the gold core in TGA (see the formulas of the two AuNPs in Table 1).

It can be seen that the two AuNPs contain almost the same total number of ca. 40 polymer chains per gold core, although the size of the gold core of AuNP-2 is larger than that of AuNP-1. This result seems to be different from the previous studies on either alkanethiol-protected[24] or water-soluble compound-protected gold nanoparticles (e.g., tiopronin[25]) and even on polymer-coated gold nanoparticles,[13] in which the number of alkanethiol ligands or polymer chains bound to a single gold core steadily increases with increasing the size of the gold core. However, this difference may be understood by taking into account two factors. First, in this study two polymers with different chain lengths were used and grafted onto the surface of the gold cores; i.e., the PS chains are longer than the PNIPAM chains (compare their molar masses or the numbers of repeating units shown in Scheme 1). Second, AuNP-2 contains twice the number of PS chains than AuNP-1. The longer chain occupies a larger space on the gold nanoparticle. The estimation of the footprints (i.e., the reciprocal of the surface chain density) of two AuNPs also supports this conclusion (Table 1). Owing to higher PS amount, AuNP-2 can be assumed to be more hydrophobic than AuNP-1. Both, however, are insoluble in water.

UV−vis spectra of both AuNPs show reasonable surface plasmon bands (SPB) with the maximum at ca. 518 nm in THF (Figure 4), consistent with our previous SPB results of PNIPAM-grafted gold nanoparticles with a similar size range.[13] The surface plasmon resonance indicates that AuNPs are well separated from each other in the good solvent THF, without any aggregation.

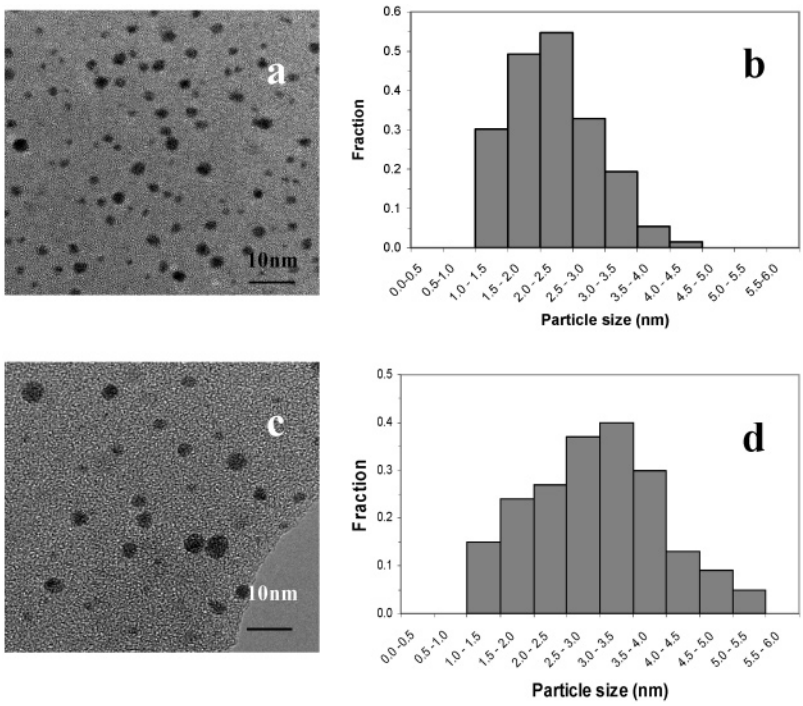

Figure 3. HRTEM images and corresponding size distributions for (a, b) AuNP-1 and (c, d) AuNP-2.

Table 1. Characterization of Both AuNP-1 and AuNP-2

amphiphilic AuNP	mean diam of Au core (nm)	no. Au atoms[a]/ shape[a]/area[a] (nm^2)	PNIPAM/PS/Au wt %[b]	formula	footprint[c]/density[c]
AuNP-1	2.5 ± 0.7	459/TO^+/24.3	57.5/17.8/24.7	$PN_{33}PS_6Au_{459}$	0.62/1.61
AuNP-2	3.0 ± 1.0	976/TO^-/40.0	34.4/26.6/39.0	$PN_{27}PS_{13}Au_{976}$	1.00/1.00

[a] The number of Au atoms per core, the shape of Au cluster, and surface area for each Au cluster were taken from refs 24 and 25. The shape model of the Au cluster was advocated by Whetten in refs 26 and 27. TO = ideal truncoctahedron (all sides equal); TO^+ = truncoctahedron in which ($0 < n - m \leq 4$), where n is the number of atoms between (111) facets and m is the number of atoms between (111) and (100) facets; TO^- = truncoctahedron in which ($-4 \leq n - m < 0$, $m > 1$). Note that owing to the presence of discernible populations in the core size histograms, the shape model and the number of Au atoms per core are all derived from the average. [b] The respective mass loss fraction of PNIPAM and PS were calculated by combining the molar grafting ratio obtained by ^1H NMR, the total mass loss fraction of the polymers gained from TGA, and the molar masses of both PNIPAM and PS. The relative amount of residual gold was directly obtained from TGA. [c] The footprint of a polymer chain = the surface area of a gold core/the number of polymer chains bound to the gold core, nm^2/chain. The surface density of polymer chains in chain/nm^2 is the inverse of the footprint. Note that the values of the footprint and the surface density are the average for both PNIPAM and PS chains.

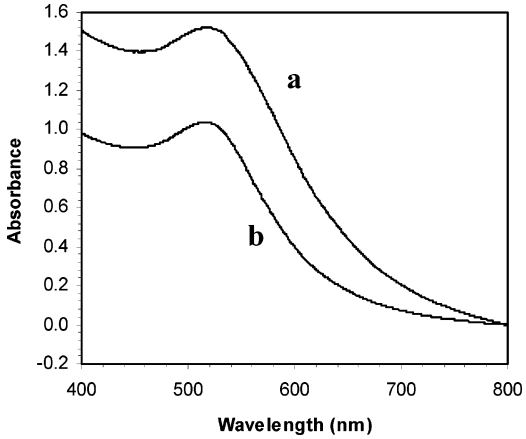

Figure 4. UV−vis spectra of (a) AuNP-1 and (b) AuNP-2.

Langmuir Monolayers of AuNPs. The polymer grafted to the gold cores consists of two types of chemically different homopolymers, PNIPAM and PS. It is known that PNIPAM is hydrophilic and water-soluble at a temperature below its lower critical solution temperature (LCST). It is also known that different morphologies and various orientations of the film-forming molecules at the air−water interface could be induced by changing the spreading solvent.[28] Saito and co-workers[28,29] reported that linear PNIPAM at the air−water interface spread from either its aqueous solution or its chloroform solution can form a stable condensed monolayer, and the deposited amount of polymer at the air−water interface spread from chloroform is larger than that spread from aqueous solution. Therefore, it can be expected that PNIPAM preferentially adsorbs at the air−water interface at the initial stage after spreading from a chloroform solution, likely due to the change in the orientation of the hydrophobic backbone of the PNIPAM chain. PS without hydrophilic groups does not spread into a monomolecular layer on the water surface because of its lacking affinity to water.[30] However, Kumaki,[30] using a very dilute solution, found that monomolecular PS particles, containing one chain only, can be obtained. Recently, comprehensive studies on the monolayers of diblock copolymers of polystyrene-*b*-poly(ethylene oxide) (PS-*b*-PEO) at the air−water interface by Langmuir film balance have been reported.[31−33] At low surface pressures, these diblock copolymers self-assemble to form surface micelles at the air−water interface, in which the PEO blocks spread on the water surface, while the PS blocks aggregate to form water-insoluble buoys at the air−water interface and tether

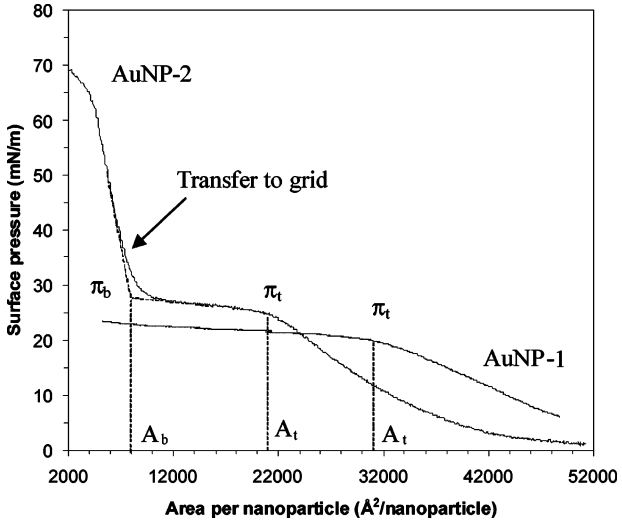

Figure 5. Compression isotherms of surface pressure vs area per nanoparticle for AuNP-1 and AuNP-2, conducted at 20 °C.

the PEO chains. Several regions that can be assigned to different polymer conformations, i.e., pancake, pancake to brush, and brush, can be recognized in the compression isotherms. The amphiphilic AuNPs are expected to spread into a film at the air−water interface at low surface pressures in a way analogous to the surface micelles self-assembled by PS-*b*-PEO on the water surface due to the similarities in their structures and properties. The PNIPAM chains tethered on a single gold core spread at the air−water interface,[28,29] whereas the PS chains simultaneously form globules which adsorb on the surface of the gold core during the evaporation of the spreading solvent, and consequently the gold PS entity acts as a water-insoluble buoy at the air−water interface.

The compression isotherms of both AuNPs are shown in Figure 5. It is interesting that the two AuNPs show quite different behaviors at the air−water interface. For AuNP-2, at large areas the grafted PNIPAM chains adsorbed at the air−water interface may be assumed to adopt a two-dimensional flattened conformation−a pancakelike structure.[31,32] The surface pressure increases steadily with film compression as the surface density of the particles increases. Below area of ca. 212 nm^2 a pseudoplateau at a surface pressure near 25 mN/m can be observed. This pseudoplateau can be associated with the dissolution of PNIPAM chains into the water subphase (forming caps) when the PNIPAM surface density exceeds a critical concentration, indicative of the onset of the transition from two to three dimensions, i.e., the pancake to brush transition.[31,32] At area lower than 80 nm^2 the isotherm shows a steep rise as the limiting area of the PNIPAM brush is reached. At this stage, the PNIPAM chains, which are tightly packed in the water subphase and anchored to the surface of the gold core, adopt a three-dimensional brush structure. Table 2 lists the isotherm parameters for both AuNPs, such as the surface pressures and the nanoparticle areas at both the onset of the pancake−brush transition (A_t and π_t) and the brush stage (A_b and π_b), respectively. These parameters were determined from the intersections of the linear fits to the corresponding adjacent regions (pancake, pancake to brush, and brush), as indicated in Figure 5. These data will be discussed later.

The isotherm of AuNP-1, on the other hand, shows an earlier occurrence of the pancake−brush transition at A_t = 313.0 nm^2, larger than A_t = 212.1 nm^2 for AuNP-2 (see Table 2 and Figure 5). Furthermore, this pseudoplateau for the AuNP-1 monolayer is much more extended compared to the AuNP-2 monolayer, and it never reaches a brush structure as occurred for the AuNP-2 monolayer. This was the case even if the AuNP-1 monolayer compression was started at a high initial surface pressure by spreading a relatively large amount of the chloroform solution containing AuNP-1 onto water surface. A probable explanation for the latter phenomenon is that the AuNP-1 dissolves into the water subphase at higher surface pressures due to its more hydrophilic character. In the case of the amphiphilic diblock copolymers PS-*b*-PEO,[31,32] the extension of the pseudoplateau increases with the length of the PEO block because the area occupied by the pancake at the onset of the pancake−brush transition is strongly dependent on the PEO length. As mentioned above, the grafted PNIPAM chains adopt a two-dimensional flattened conformation at the air−water interface prior to the onset of the pancake−brush transition and are assumed to have a more compact structure at the air−water interface as observed for the PEO chains in the pancake structure.[32] Therefore, the PNIPAM length (L_t) at the onset of the pancake−brush transition can be estimated from the nanoparticle area at the transition point A_t by $L_t = (A_t/\pi)^{1/2} - D/2$, where D is the diameter of the gold core, listed in Table 2 for both AuNPs. It is evident that the PNIPAM chains in the AuNP-1 are 2 nm longer than those in the AuNP-2, indicating that the PNIPAM chains in the AuNP-1 monolayer are more stretched at the air−water interface than those in the AuNP-2 monolayer. Comparing with the length of a fully stretched PNIPAM chain, ca. 13.8 nm, and assuming that the PNIPAM backbone adopts an all-trans conformation, we can conclude that the PNIPAM chains for both AuNPs adopt a more extended conformation at the air−water interface at the transition stage, and the PNIPAM chain lengths are as large as about half-length of the fully stretched PNIPAM. An analogous result was reported by Ohno for poly(methyl methacrylate)-coated gold nanoparticles.[18] The PNIPAM chain lengths for both AuNPs at the air−water interface may also be compared with the profile length of the grafted PNIPAM and PS on the AuNP-2. The latter can be estimated to be (13.0 nm − 3.0 nm of the size of the gold core)/2 = 5.0 nm, where the value of 13 nm is the diameter of the PNIPAM/PS−AuNP-2 dissolved in the good solvent THF and determined by DLS. Evidently, the PNIPAM chain lengths for both AuNPs at the air−water interface are higher than that for AuNP-2 in solution. This phenomenon may be interpreted as a result of the strong anisotropic interactions among polymer chains arising from the high surface density.[18] In the THF, which is a good solvent, for both PNIPAM and PS chains, the polymer brush grafted onto the spherical surface of the gold core have a large space to swell in three dimensions. The polymer density decreases with increasing distance from the core center. As a result, the anisotropic interaction that causes the chain extension will get weaker in the outmost layer of the polymer brush than that close to the gold core. The outmost polymer chains, therefore, likely adopt a coil structure, although the interior chains close to the gold core are more extended. However, at the air−water

Table 2. Overview of Parameters Measured with Compression Isotherms for Both AuNPs

amphiphilic AuNP	π_t/mN/m	A_t/nm^2	π_b/mN/m	A_b/nm^2	L_t/nm	L_b/nm
AuNP-1	20.5	313.0			8.7	
AuNP-2	25.3	212.1	28.0	80.0	6.7	3.54

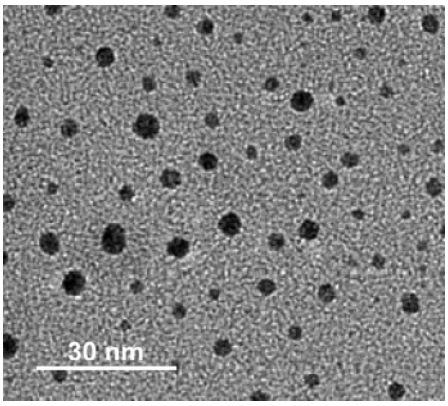

Figure 6. HRTEM image of transferred Langmuir monolayer of AuNP-2.

interface where the amphiphilic gold nanoparticles are spread, only the PNIPAM chains can swell in two dimensions, whereas the collapsed PS chains aggregate toward the gold core, this resulting in a large repulsive effect of PS on PNIPAM. Assuming that most of the PNIPAM chains preferentially adsorb on the water surface,[28,29] the PNIPAM surface density is expected to be higher than that in THF, which causes a higher anisotropic interaction between the PNIPAM chains at the air−water interface.

To illustrate the formation of a monolayer instead of a multilayer for the AuNP-2, the AuNP-2 film was transferred onto a carbon-coated TEM grid by Schaefer deposition at $\pi = 35$ mN/m in the brush region ($\pi_b = 28.0$ mN/m) (see Figure 5). The TEM image is shown in Figure 6. We can see that the gold cores are well separated in the film with no overlapping and that their diameters are within the corresponding distribution width of Figure 3d. This shows that a monolayer of the AuNP-2 forms at the air−water interface. On the other hand, the analysis of the limiting area of nanoparticles in the brush stage (i.e., the brush area) from the isotherm of the AuNP-2 also supports this point. From the brush area of the AuNP-2, $A_b = 80.0$ nm^2 (at $\pi_b = 28.0$ mN/m), the diameter (D) of these particles can be calculated to be $D = 10.1$ nm according to $A_b = \pi(D/2)^2$, much larger than the diameter of the gold cores of 3.0 ± 1.0 nm. The length of the grafted polymer (L_b) can further be obtained from the nanoparticle diameter D to be 3.54 nm, about a half of the PNIPAM chain length (L_t) of 6.7 nm at the pancake−brush transition. This means that about half length of each PNIPAM chain dives into the water subphase, avoiding overlapping with each other,[31−33] and the other half is still at the air−water interface, during compression from the onset of the pancake−brush transition to the initial brush stage. The characteristic of the PNIPAM chains in the brush region is very significant because the deposition of the AuNP-2 monolayer onto substrate was conducted at $\pi = 35$ mN/m in the brush region and followed by the contact angle measurements. Similarly, at $\pi = 35$ mN/m ($A = 75.0$ nm^2) in the isotherm, the particle diameter and the length of the grafted polymer can also be estimated to be 10.0 and 3.5 nm, very close to those at $\pi_b = 28.0$ mN/m ($A_b = 80.0$ nm^2).

Table 3. Contact Angles on Different Surfaces

surface	contact angle/deg: literature data	contact angle/deg: measured
PS film [ref 38]	90.93 ± 0.32[a]	
PS film [ref 39]	88.42 ± 0.28[a]	
PS film [ref 40]	86 ± 1[a]	
PNIPAM brush [ref 41]	84 ± 5[a]	
PNIPAM brush [ref 42]	66[a]	
surface L		82 ± 2[b]
surface D		77 ± 2[b]

[a] Advancing contact angle. [b] Sessile contact angle.

It is worth noting that the temperature at which the Langmuir experiment is carried out significantly affects the shape of the isotherm of the monolayer for these amphiphilic gold nanoparticles because the grafted PNIPAM chains are thermally sensitive and the conformation of the PNIPAM chains greatly varies with temperature. A more extensive study of the Langmuir monolayers of the amphiphilic gold nanoparticles as a function of subphase temperature is of considerable interest and is still under progress.

Contact Angle Measurements and Distribution of PNIPAM and PS Chains. Chemically different polymers do not usually mix with each other. In the case of PS-*b*-PNIPAM diblock copolymers, it has been observed that the two blocks are totally phase separated.[34] Thus, it may be assumed that PS and PNIPAM chains are not randomly distributed on the surface of the gold cores but form phase-separated regions. This, however, is extremely difficult to verify experimentally. Brewer and Leggett[35] have recently given an evidence for the phase separation of the mixed self-assembled monolayers (SAM) formed by the coadsorption of hydroxyl- and methyl-terminated alkanethiols with similar chain length on a bulk gold surface by means of friction force microscopy and chemical force microscopy. In this work, contact angle measurement and X-ray photoelectron spectroscopy (XPS) were conducted on both the upper and lower surfaces of the monolayer for AuNP-2. Actually, the XPS measurement did not show any difference in the surface composition for both upper and lower surfaces of the Langmuir monolayer, probably due to the instrumental limitations (analysis depth of 2−10 nm), to the interference from the SiO_2 substrate, and to the pretreatment.[36]

If both PNIPAM and PS chains would be homogeneously distributed on the surface of the gold core, one could expect that the contact angles of a sessile water drop on both surface L and surface D would be the same. If there is any phase separation of PNIPAM and PS on the gold core such that it becomes amphiphilic, then the contact angles on surface L and surface D could be different. Thus, a hydrophilic transfer would lead to a more hydrophobic surface (i.e., surface L) and a hydrophobic transfer to a more hydrophilic one (i.e., surface D), following the general rules of LB transfer. Table 3 lists the sessile drop contact angles of water on both surface L and surface D, respectively. It can be seen that the contact angle on surface L is ca. 5° higher than that on surface D. Thus, surface L shows a more hydrophobic character than surface D.

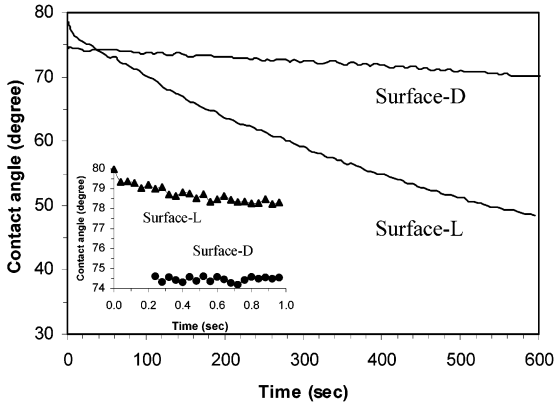

Figure 7. Time dependence of the contact angle of water on surfaces D and L. Inset shows the initial contact angle within 1.0 s (black triangle for surface L and black dot for surface D).

It should be pointed out that the seemingly simple contact angle phenomena, however, are very complicated. The contact angle can be affected by many factors, such as interfacial tension, chemical heterogeneity, surface roughness, molecular orientation, and reorganization.[37] For the same material, the contact angle values are also much dependent on the procedure of the film preparation and the technique applied to measure the contact angle,[38] e.g., the sessile drop contact angle or the dynamic contact angle (advancing and receding contact angles) measurement technique. It is also known that the dynamic contact angle at low advancing speed is often, but not always, identical to the static contact angle.[38] Table 3 also lists some literature data of advancing contact angles[38−42] measured at low advancing speed for PS film and PNIPAM brush. By comparing the literature data of the advancing contact angles of water on the PS films (Table 3), with the sessile drop contact angle of 82 ± 2° on surface L measured in this study, it is evident that surface L is not as hydrophobic as the pure PS film but shows a slightly hydrophilic nature. This may be speculated to be due to the coexistence of both the PNIPAM and PS chains on surface L. As discussed above, about half length of PNIPAM chains for AuNP-2 is still at the air−water interface in the brush region and thus coexists with the collapsed PS chains on surface L, after the hydrophilic transfer is performed. This part of the PNIPAM chains starts to reorganize and dissolves rapidly into a water drop when the contact angle measurement is conducted on surface L at room temperature, which results in a slightly hydrophilic character of surface-L. On the other hand, by reference to the literature data of advancing contact angles of water on the PNIPAM brushes (Table 3), measured at room temperature, the sessile contact angle of 77 ± 2° on surface D is just the average of the literature data. The literature data even scattered considerably, perhaps due to the complexity of the contact angle phenomenon as noted above. However, the sessile contact angle is very comparable to ∼75° of water on the LB surface of the diblock copolymer poly(γ-benzyl L-glutamate)-*b*-PNIPAM.[43]

Figure 7 shows the dynamic behavior of the contact angle vs time. The contact angle of water on surface L decreases rapidly with time. In particular, in the initial period within 1 s (see the inset of Figure 7, the data were obtained by video captures with a time interval of 0.04 s and subsequent image analysis by ADSA), the contact angle on surface L drops from 80° to 78°, most likely due to the reorganization/dissolution of the PNIPAM chains spread in the monolayer into a water droplet, and subsequently the hydrophilic substrate surface is disclosed to the water droplet, leading to a further decrease in the contact angle. However, it is still clear that surface L shows a hydrophobic nature in the initial stage. On surface D, on the other hand, the contact angle decreases only slightly over the entire time range in Figure 7. This indicates that the hydrophilic nature of surface D due to the PNIPAM coverage. With the reorganization of the PNIPAM chains, the disclosed hydrophobic substrate surface will interfere with a decrease in contact angle.

As a result of the contact angle measurements, we can see that both PNIPAM and PS chains tend to be unevenly distributed on the surface of the gold cores; in other words, the phase separation may occur between PNIPAM and PS chains, although the preparation of the gold nanoparticles takes place in a homogeneous phase.

Conclusions

Amphiphilic gold nanoparticles grafted with different ratios of the PNIPAM and PS chains were successfully prepared. The AuNP-2 compression isotherm shows different stages associated with the variance of PNIPAM conformations at the air−water interface, while the AuNP-1 monolayer only shows an extended pseudoplateau with no ability to reach a brush structure. Furthermore, the contact angle measurements on the upper and lower surfaces of the AuNP-2 monolayer revealed that one surface deposited by hydrophilic transfer shows a more hydrophobic character than the other obtained by hydrophobic transfer. This implies that the phase separation between PNIPAM and PS on the surface of the gold cores may occur.

Acknowledgment. We thank the Finnish Technology Agency for financial support. We are grateful to Dr. Leena-Sisko Johansson, Center for Chemical Analysis, Helsinki University of Technology, for help with XPS measurements.

References and Notes

(1) Shiway, A. N.; Katz, E.; Willner, I. *ChemPhysChem* **2000**, *1*, 18−52.
(2) Remacle, F.; Levine, R. D. *ChemPhysChem* **2001**, *2*, 20−36.
(3) Templeton, A. C.; Wuelfing, W. P.; Murray, R. W. *Acc. Chem. Res.* **2000**, *33*, 27−36.
(4) Cortie, M. *Gold Bull.* **2003**, *36*, 74.
(5) Brust, M.; Walker, M.; Bethell, D.; Schiffrin, D. J.; Whyman, R. *J. Chem. Soc., Chem. Commun.* **1994**, 801−802.
(6) Ohno, K.; Koh, K.-M.; Tsujii, Y.; Fukuda, T. *Macromolecules* **2002**, *35*, 8989−8993.
(7) Mandal, T. K.; Fleming, M. S.; Walt, D. R. *Nano Lett.* **2002**, *2*, 3−7.
(8) Nuss, S.; Böttcher, H.; Wurm, H.; Hallensleben, M. L. *Angew. Chem., Int. Ed.* **2001**, *40*, 4016−4018.
(9) Raula, J.; Shan, J.; Nuopponen, M.; Niskanen, A.; Jiang, H.; Kauppinen, E.; Tenhu, H. *Langmuir* **2003**, *19*, 3499−3504.
(10) Wuelfing, W. P.; Gross, S. M.; Miles, D. T.; Murray, R. W. *J. Am. Chem. Soc.* **1998**, *120*, 12696−12697.
(11) Corbierre, M. K.; Cameron, N. S.; Sutton, M.; Mochrie, S. G. J.; Lurio, L. B.; Ruhm, A.; Lennox, R. B. *J. Am. Chem. Soc.* **2001**, *123*, 10411−10412.
(12) Mangeney, C.; Ferrage, F.; Aujard, I.; Marchi-Artznern, V.; Jullien, L.; Ouari, O.; Rekai, E. D.; Laschewsky, A.; Vikholm, I.; Sadowski, J. W. *J. Am. Chem. Soc.* **2002**, *124*, 5811−5821.
(13) Shan, J.; Nuopponen, M.; Jiang, H.; Kauppinen, E.; Tenhu, H. *Macromolecules* **2003**, *36*, 4526−4533.

(14) Lowe, A. B.; Sumerlin, B. S.; Donovan, M. S.; McCormick, C. L. *J. Am. Chem. Soc.* **2002**, *124*, 11562−11563.
(15) Brust, M.; Kiely, C. J. *Colloids Surf. A* **2002**, *202*, 175−186.
(16) Huang, S.; Minami, K.; Sakaue, H.; Shingubara, S.; Takahagi, T. *Langmuir* **2004**, *20*, 2274−2276.
(17) Brown, J. J.; Porter, J. A.; Daghlian, C. P.; Gibson, U. J. *Langmuir* **2001**, *17*, 7966.
(18) Ohno, K.; Koh, K.; Tsujii, Y.; Fukuda, T. *Angew. Chem., Int. Ed.* **2003**, *42*, 2751−2754.
(19) Yang, Y.; Pradhan, S.; Chen, S. *J. Am. Chem. Soc.* **2004**, *126*, 76−77.
(20) Mitsukami, Y.; Donovan, M. S.; Lowe, A. B.; McCormick, C. L. *Macromolecules* **2001**, *34*, 2248−2256.
(21) Thang, S. H.; Chong, Y. K.; Mayadunne, R. T. A.; Moad, G.; Rizzardo, E. *Tetrahedron Lett.* **1999**, *40*, 2435−2438.
(22) Ganachaud, F.; Monteiro, M. J.; Gilbert, R. G.; Dourges, M.-A.; Thang, S. H.; Rizzardo, E. *Macromolecules* **2000**, *33*, 6738−6745.
(23) Zeng, F.; Tong, Z. *Polymer* **1997**, *38*, 5539−5544.
(24) Hostetler, M. J.; Wingate, J. E.; Zhong, C.-Z.; Harris, J. E.; Vachet, R. W.; Clark, M. R.; Londono, J. D.; Green, S. J.; Stokes, J. J.; Wignall, G. D.; Glish, G. L.; Porter, M. D.; Evans, N. D.; Murray, R. W. *Langmuir* **1998**, *14*, 17−30.
(25) Templeton, A. C.; Chen, S.; Gross, S. M.; Murray, R. W. *Langmuir* **1999**, *15*, 66−76.
(26) Whetten, R. L.; Khoury, J. T.; Alvarez, M. M.; Murthy, S.; Vezmar, I.; Wang, Z. L.; Stephen, P. W.; Cleveland, C. L.; Luedtke, W. D.; Landman, U. *Adv. Mater.* **1996**, *5*, 428−433.
(27) Whetten, R. L.; Shafigullin, M. N.; Khoury, J. T.; Schaaff, T. G.; Vezmar, I.; Alvarez, M. M.; Wilkinson, A. *Acc. Chem. Res.* **1999**, *32*, 397−406.
(28) Saito, W.; Kawaguchi, M.; Kato, T.; Imae, T. *Langmuir* **1996**, *12*, 5947−5950.
(29) Kawaguchi, M.; Yamamoto, M.; Kato, T. *Langmuir* **1998**, *14*, 2582−2584.
(30) Kumaki, J. *Macromolecules* **1988**, *21*, 749−755.
(31) Baker, S. M.; Leach, K. A.; Devereaux, C. E.; Gragson, D. E. *Macromolecules* **2000**, *33*, 5432−5436.
(32) Goncalves da Silva, A. M.; Filipe, E. J. M. *Langmuir* **1996**, *12*, 6547−6553.
(33) Bijsterbosch, H. D.; de Haan, V. O.; de Graaf, A. W.; Mellema, M.; Leermakers, F. A. M.; Cohen Stuart, M. A.; van Well, A. A. *Langmuir* **1995**, *11*, 4467−4473.
(34) Nuopponen, M.; Ojala, J.; Tenhu, H. *Polymer* **2004**, *45*, 3643−3650.
(35) Brewer, N. J.; Leggett, G. J. *Langmuir* **2004**, *20*, 4109−4115.
(36) We did not measure the thickness of the monolayer of the amphiphilic gold nanoparticles on substrate. It is believed to be very thin, likely about or below 2 nm, according to the low molar masses of the PNIPAM and PS used in the preparation of the gold nanoparticles. It was confirmed with the N 1s signals for both upper and lower surfaces in the XPS measurements that no background of the N 1s signals was observed. In contrast, the background of the Si 2p signals revealed that all Si signals came from the SiO_2 substrate, were covered by the monolayer, and showed the identical compositions for both surfaces in several XPS measurements.
(37) Kwok, D. Y.; Neumann, A. W. *Adv. Colloid Interface Sci.* **1999**, *81*, 167−249.
(38) Augsburg, A.; Grundke, K.; Pöschel, K.; Jacobasch, H.-J.; Neumann, A. W. *Acta Polym.* **1998**, *49*, 417−426.
(39) Kwok, D. Y.; Lam, C. N. C.; Zhu, K.; Wu, R.; Neumann, A. W. *Polym. Eng. Sci.* **1998**, *38*, 1675−1684.
(40) Craig, R. G.; Berry, G. C.; Peyton, F. A. *J. Phys. Chem.* **1960**, *64*, 541−543.
(41) Volpe, C. D.; Cassinelli, C.; Morra, M. *Langmuir* **1998**, *14*, 4650−4656.
(42) Balamurugan, S.; Mendez, S.; Balamurugan, S. S.; O'Brien, M. J., II; Lopez, G. P. *Langmuir* **2003**, *19*, 2545−2549.
(43) Shimojo, S.; Akaike, T.; Hara, M.; Higuchi, A.; Park, I.-K.; Cho, C.-S. *J. Biomater. Sci., Polym. Ed.* **2002**, *13*, 829−841.

MA049269J